JPhys Materials

PAPER • OPEN ACCESS

Efficient and selective glycerol electrolysis for the co-production of lactic acid and hydrogen with multi-component Pt/C-zeolite catalyst

To cite this article: Muhammad Aslam *et al* 2024 *J. Phys. Mater.* **7** 015002

IOP Publishing J. Phys. Mater. 7 (2024) 015002 https://doi.org/10.1088/2515-7639/ad0561

Journal of Physics: Materials

OPEN ACCESS

RECEIVED
31 July 2023

REVISED
29 September 2023

ACCEPTED FOR PUBLICATION
20 October 2023

PUBLISHED
9 November 2023

PAPER

Efficient and selective glycerol electrolysis for the co-production of lactic acid and hydrogen with multi-component Pt/C-zeolite catalyst

Muhammad Aslam[1], **Miriam Navlani-García**[2], **Diego Cazorla-Amorós**[2] and **Hui Luo**[1,3,*]

[1] Department of Chemical Engineering, Imperial College London, South Kensington Campus, SW7 2AZ London, United Kingdom
[2] Materials Science Institute and Inorganic Chemistry Department, University of Alicante, Ap. 99, E-03080 Alicante, Spain
[3] School of Mechanical Engineering Sciences, University of Surrey, Stag Hill Campus, GU2 7XH Guildford, United Kingdom
[*] Author to whom any correspondence should be addressed.

E-mail: hui_luo@surrey.ac.uk

Keywords: glycerol oxidation, electrolysis, lactic acid, hydrogen production

Abstract

Among various electrochemical reactions to produce fuels and chemicals, glycerol electrolysis to co-produce hydrogen and lactic acid has received great attention. However, studies have shown the benchmark Pt based catalysts are insufficient in selectively catalysing the glycerol to lactic acid transformation, resulting in a low yield of lactic acid. Here we report a study on glycerol electrolysis with anion-exchange membrane electrode assembly electrolyser. The reaction conditions including mass transport, temperature, current density and KOH concentration were optimised, among which temperature played a significant role in facilitating the reaction rate and thermodynamics. With the optimised condition a multicomponent Pt/C-zeolite electrocatalyst system (Pt/C-CBV600) was developed and tested, which is capable to increase the lactic acid selectivity to 57.3% from the 33.8% with standalone Pt/C. Although the detailed mechanism required further investigation, it is hypothesised that the CBV600 zeolite with abundant Lewis acid surface sites can effectively bind the dihydroxyacetone intermediate, and drive the reaction towards pyruvaldehyde heterogeneously, the key step to form lactic acid.

1. Introduction

The concept of power-to-X (X = fuels, chemicals) developed in recent years has opened up a new research focus on combining energy storage with chemical conversion. The electrochemical transformation of low-value feedstocks to produce high energy-density clean fuels and commodity chemicals is particularly attractive due to the added economic value and environmental impact via decarbonizing the energy and chemical sectors [1, 2]. During the search for suitable electrochemical reactions, glycerol electrolysis to co-produce hydrogen and bio-chemicals have received significant attentions [3–6]. Since glycerol is a waste by-product from the biodiesel industry with a surplus supply of 4.66 Mt annually, it is an ideal feedstock to valorise [7]. Among the various glycerol derivatives, lactic acid, the monomer for the flagship bio-polymer poly-lactic acid, benefits from the largest market size among the five most expensive listed glycerol derivatives, presenting a lucrative business opportunity [8].

Traditionally, more than 90% of lactic acid is produced via anaerobic fermentation of sugars, such as glucose. The main issues associated with this production method are cost and environmental impact due to the strict reaction conditions (pH 5–7, temperature < 40 °C) and waste materials such as $CaSO_4$ produced in downstream purification and separation [8–12]. Besides, the low productivity (1–13 $\mathrm{g\,l^{-1}\,h^{-1}}$) also limits the scaling up of manufacturing [13]. Our strategy to tackle this challenge is to develop a glycerol electrolysis system that can continuously produce hydrogen and lactic acid simultaneously, with direct utilization of increasingly available renewable electricity and under mild conditions.

A survey of prior literature reveals that the glycerol to lactic acid conversion undergoes a dehydrogenation-dehydration-Cannizzaro solution phase reaction pathway in alkaline media, with the

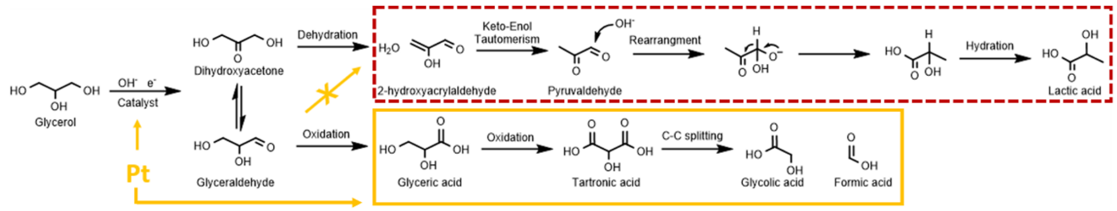

Figure 1. Glycerol dual reaction pathway: dehydration vs. oxidation. Pt-based electrocatalysts can effectively catalyze the glycerol → dihydroxyacetone/glyceraldehyde step as well as the following deprotonation/C–C cleavage steps [14, 16, 21].

competing reaction being the typically electrochemical partial oxidation via glyceric acid, as illustrated in figure 1 [14–16]. It can be seen that glycerol first undergoes electrooxidation into two isomers—glyceraldehyde and dihydroxyacetone. Consequently, the two isomers are consumed through two competing reaction pathways. In the first pathway, dihydroxyacetone is dehydrated into pyruvaldehyde, which is then transformed into lactic acid through an intramolecular Cannizzaro reaction [17]. In this reaction, pyruvaldehyde first undergoes benzylic acid rearrangement under base catalysis and is then hydrated to form lactic acid [15]. According to Albuquerque *et al*, this is a well-understood process where the rearrangement of α-keto aldehydes, such as pyruvaldehyde, into α-hydroxy carboxylic acids, such as lactic acid, is favored by alkaline media as well as the presence of Lewis acids [18]. In the alternative pathway, glyceraldehyde is oxidised into glyceric acid, which can in turn be further oxidised once more to form tartronic acid. The latter can then undergo a split of its C–C bond to form glycolic and formic acids [19]. Pt-based electrocatalysts have been known to be the most active in catalysing the glycerol transformation, yet it also primarily drives the competing electrochemical oxidation pathway, and therefore unfavorable to the production of lactic acid [14–16, 20]. Here, our goal is to discover new electrocatalyst systems for lactic acid production, exhibiting an unprecedented combination of activity and selectivity.

It has been reported that in heterogeneous catalysis, Lewis acid sites from certain inorganic materials, such as ZrO_2, [18] Al_2O_3 [22] as well as Lewis acidic zeolites [23, 24] can mediate the dihydroxyacetone to pyruvaldehyde chemical transformation process, by coordinating the carbonyl and hydroxyl groups, thus accelerating the keto-enol tautomerisation and dehydration of the component [25, 26]. Subsequently, the pyruvaldehyde will diffuse into the solution, where the OH^- ions can catalyze the Cannizzaro reaction and form finally the lactic acid. In CO_2 reduction reaction, the concept of tandem mechanism has been considered a promising strategy to tailor the catalytic microenvironment, where two or more distinct catalytic sites are closely located to achieve sequential processes, that can improve the catalytic activity and tune the selectivity towards C_{2+} products [27–30]. By fabricating micropatterned electrodes containing Cu and Au/Ag, Lum and Ager demonstrated that the sequential process can be affected on the micron scale, with the diffusional transport of intermediates in the liquid phase [31]. Since glycerol to dihydroxyacetone is an electrochemical step, and Pt is the most active catalyst, if a tandem multicomponent catalyst system containing Pt sites and catalyst materials with Lewis acid sites can be designed, the possibility to increase the selectivity towards lactic acid can be achieved from simplifying the reaction as:

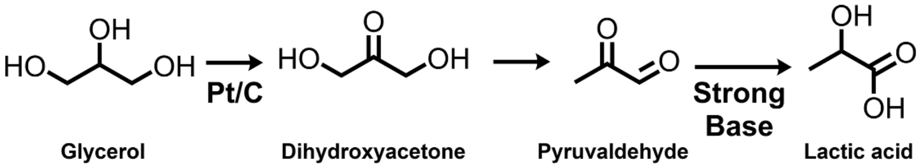

Because zeolite materials have shown high selectivity in catalysing dihydroxyacetone towards lactic acid in previous studies, here we chose to combine it with the Pt/C to construct a multi-component system. We fabricated the Pt/C-zeolite (CBV600) electrodes and characterized the composition, structure and surface properties *ex-situ*, followed by testing it electrochemically in a modified MEA glycerol electrolyser. With the optimised reaction conditions, we are able to achieve a lactic acid yield of 57.3%, with a 99.4% H_2 production faradaic efficiency on the cathode.

2. Methods

2.1. Materials

Platinum nanoparticles 60 wt.% on carbon (Pt/C) (HiSPEC 9100) and Vulcan XC 72 R carbon black were obtained from fuel cell store. Zeolite Y CBV 600 was purchased from Zeolyst. Glycerol (⩾99.0%), potassium hydroxide (KOH) (pellets, 99.99% excl sodium content) and sulfuric acid (H_2SO_4) (99.999%) were obtained from Sigma Aldrich. Nafion® (D-521 dispersion, 5% w/w in water and 1-propanol) was obtained from Alpha Aesar and ethanol absolute (⩾99.8%) was obtained from VWR Chemicals.

2.2. Electrode preparation and characterisation

The catalyst inks were prepared by dispersing 3 mg of Pt/C and 9 mg of carbon black (for Pt/C electrode) or CBV 600 zeolite (for Pt/C-CBV600) in 4200 μl water, 1584 μl ethanol and 216 μl 5 wt % Nafion solution, followed by probe sonication for 10 min. The catalyst inks were spray coated onto the carbon paper (Freudenberg H23) with 3 cm × 3 cm dimension to achieve 0.1 mg cm^{-2} Pt loading in the anode. The same Pt/C ink was used to prepare the cathode with 2.5 cm × 2.5 cm area and 0.05 mg cm^{-2} Pt loading.

High-resolution transmission electron microscopy (HR-TEM) images were obtained by a FEI Titan 80/300 at an operating voltage of 300 kV. The x-ray diffraction (XRD) patterns were performed using PANanalytical's X'PERTPRO x-ray diffractometer with Ni filtered Cu Kα radiation and an X'Celerator multistrip detector. The scanned two theta ranges from 15° to 90° at 30° min^{-1}. To reduce the noise in the final signal, the sample holder was rotating at 90° per second. N_2 sorption isotherms were conducted at −196 °C with data collected from a pressure range 10^{-5}–0.99 in micromeritics 3Flex system with ∼10 mg of degassed sample (200 °C overnight). The brunauer-emmett-teller (BET) surface area was deduced from the adsorption isotherm in the relative pressure range of <0.03.

Temperature-programmed desorption of ammonia (NH_3–TPD) experiments were performed in a thermogravimetric analysis coupled differential scanning calorimetry (TGA-DSC) instrument (TA Instruments, SDT Q600 Simultaneous) coupled to a mass spectrometer (Thermostar, Balzers, BSC 200). Before the adsorption of NH_3, the samples (0.01 g) were pre-treated in a He atmosphere at 400 °C (heating rate of 20 °C min^{-1}) for 30 min. After that, the temperature was cooled down to 100 °C and the samples were saturated in a stream of 5% NH_3–He (60 ml min^{-1}) for 25 min. Afterwards, the gas stream was changed to He (60 ml min^{-1}) and the temperature was kept at 100 °C for 60 min. The total NH_3 adsorbed by the samples was calculated from the total mass uptake registered upon introducing NH_3 in the system. Lewis acid sites were determined from the difference between the total NH_3 adsorbed, determined when the sample was in contact with the NH_3-He mixture, and the most weakly adsorbed NH_3 determined from the fast weight loss observed after switching from the NH_3-He mixture to He at 100 °C.

2.3. Electrolysis testing and product analysis

Electrolysis measurements were performed with a Metrohm Autolab potentiostat for 1 h with 1 M glycerol/KOH as anolyte and KOH as catholyte. The reaction conditions, such as electrolyte flow rate, temperature, electrolysis current and KOH concentration were varied as detailed in the discussion below. The H_2 produced at the cathode was quantified in real time with an Agilent 7890B gas chromatography. At the end of the experiments, the products accumulated in the anode chamber were quantified using Agilent 1260 infinity II high-performance liquid chromatography. The results have been calculated according to the equations listed below:

$$\text{Product yield }\% = \frac{\text{product X in mole}}{\text{consumed glycerol in mole}} \times 100\%$$

$$\text{Glycerol Conversion }\% = \frac{\text{consumed glycerol in mole}}{\text{initial glycerol in mole}} \times 100\%$$

$$\text{Faradaic efficiency} = \frac{\text{mole of product formed } \times nF}{\text{total charge passed}} \times 100\%,$$

where F is the faradaic constant (96 485 C mol^{-1}) and n is the electron transfer number.

3. Results and discussion

The morphology of the Pt/C and Pt/C-CBV600 catalysts was first investigated with TEM and XRD. As shown in the TEM images (figure 2), the CBV600 zeolite nanoparticles are 400–500 nm in size, with mesoporous structure and a surface area of 656 m^2 g^{-1}, measured from BET. The morphology of the commercial Pt/C nanoparticles exhibits a face-centred cubic structure and a diameter of 3–5 nm, with a typical interplanar spacing for pure Pt {111} planes (0.231 nm). These observations are in line with the results obtained from XRD (figure 3(a)), where three main peaks indexed to (111), (200) and (220) planes are presented

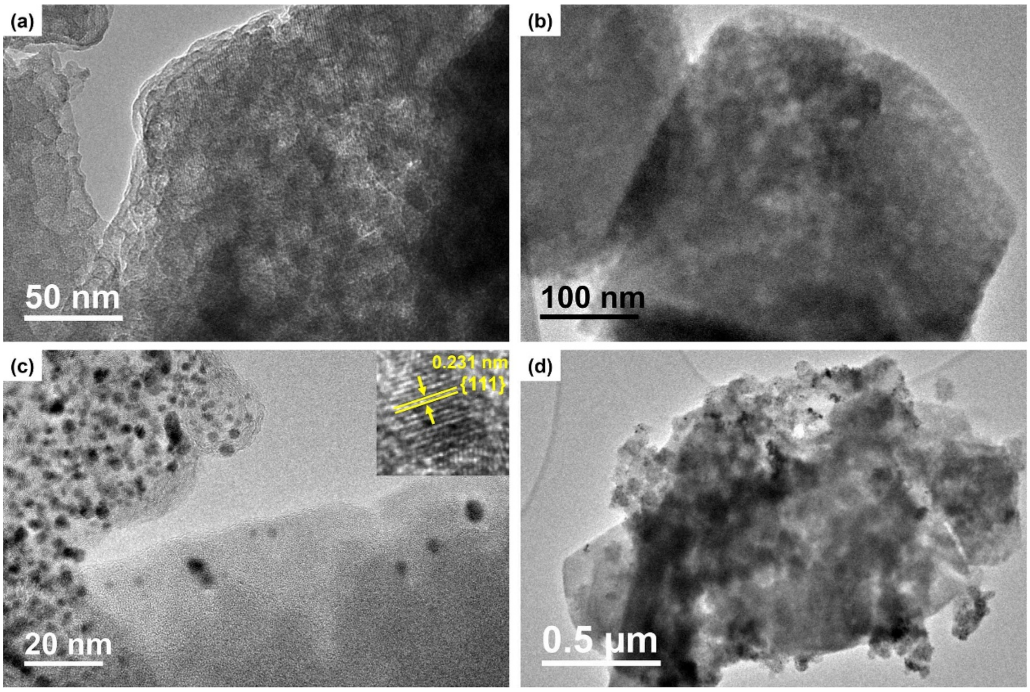

Figure 2. The morphology of CBV600 zeolite (a), (b) and Pt/C-CBV600 (c), (d) catalyst. (Insert (c)). High-resolution Pt nanoparticle image with d-spacing of 0.231 nm, corresponding to Pt {111} plane).

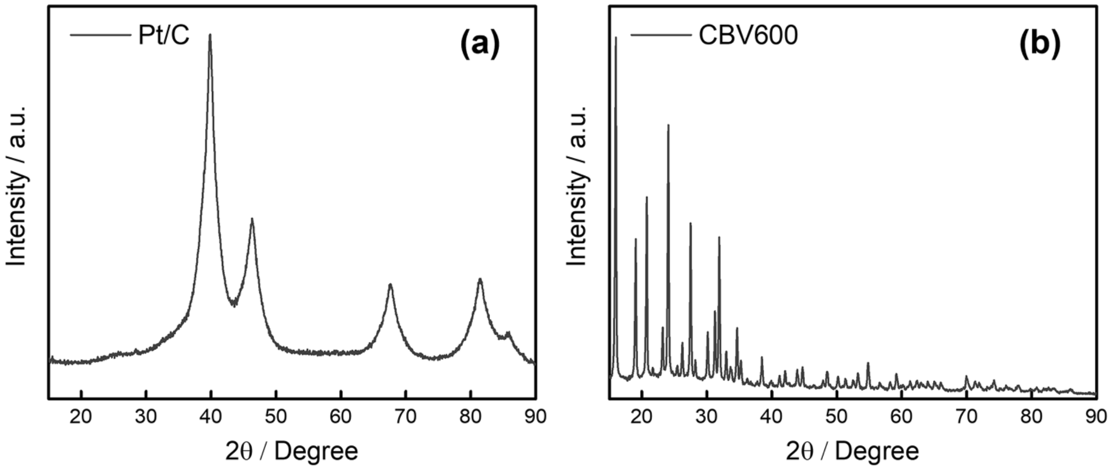

Figure 3. XRD patterns of (a) Pt/C and (b) CBV 600 zeolite.

(PCPDFWIN #70−2431). The Pt/C catalysts are well supported on the zeolite nanoparticles, providing good contact for charge and mass transport.

Next, we initiated the glycerol electrolysis study over the commercial Pt/C catalyst as the anode material, by exploring the optimal reaction condition. Four major reaction parameters were identified that may affect the selectivity towards lactic acid, and hereby investigated, namely electrolyte flow rate, electrolysis current, operation temperature, as well as KOH concentration. First, standard conditions for each parameter were selected as a starting point, as shown in figure 4. Then, control experiments were conducted to each parameter.

As can be seen from figure 5, among all four parameters, apart from electrolysis current, all parameters showed a positive effect on the lactic acid yield, with temperature and KOH concentration having the most important influences. By increasing the operation temperature from 20 to 60 °C, the lactic acid yield improved from 17.4% to 35.4%. Similarly, increasing KOH concentration from 1 M to 3 M resulted in a yield increase from 16.8% to 29.3%. Current, on the contrary, showed a very minor effect, with the lactic acid yield

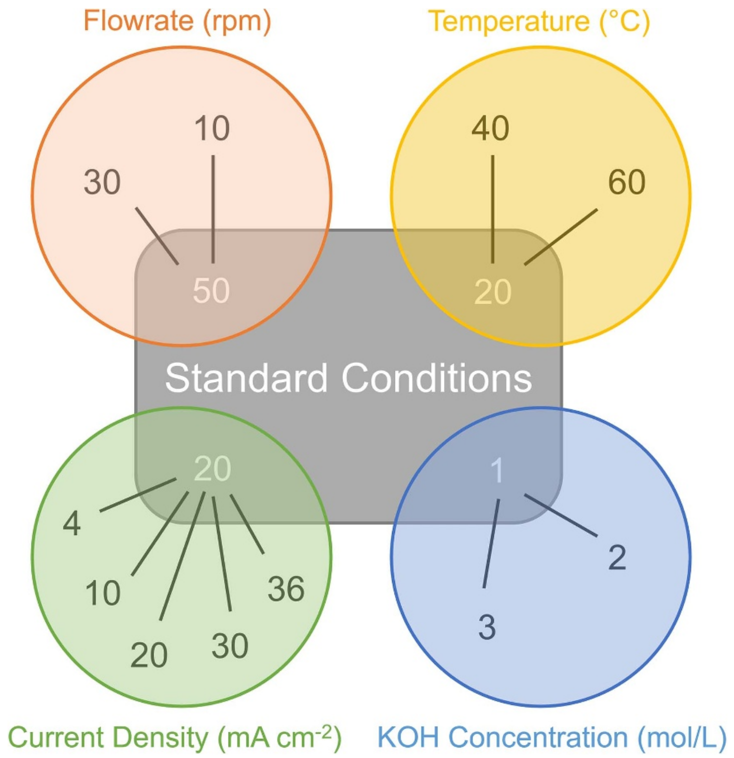

Figure 4. Reaction parameters used for the optimisation step: flow rate: 10, 30, 50 rpm; temperature: room (20), 40, 60 °C; current density: 4, 10, 20, 24, 30, 36 mA cm^{-2}; KOH concentration: 1, 2, 3 mol l^{-1}. Standard condition: 50 rpm, room temperature (20 °C), 100 mA (20 mA cm^{-2}) and KOH 1 mol l^{-1}.

peaking at 20 mA cm^{-2} (17.4%). To understand these behaviors, it is necessary to combine them with the glycerol dehydration mechanism discussed before.

Since the glycerol to lactic acid transformation is a combined electrochemical and chemical step, the reaction pathway is governed by factors that are involved in both reaction processes. Flow rate affects the mass transport of glycerol reactants and products to and from the catalyst surface, which can significantly impact the reaction rate in both electrochemical and heterogeneous catalysis. Diffusion limitations or inadequate flow conditions can reduce the overall catalytic activity by limiting the access of reactant molecules to the catalyst surface or hindering the removal of reaction products. In this case, at low mass transport, the accessibility to Pt active sites is limited, leading to lower reactivity and glycerol conversion rate. Besides, low mass transport results in the dihydroxyactone and glyceraldehyde intermediates hard to desorb from the Pt surface, which on the one hand, limits the chemical dehydration of dihydroxyactone, [16] while on the other hand, promotes the over electrooxidation of the glyceraldehyde towards glyceric acid and other oxidation products [32–34].

Current in a galvanostatic control mode affects the overpotentials that drive the glycerol oxidation process, which has previously been demonstrated to have an impact on glycerol oxidation selectivity [19, 35, 36]. At low overpotentials (i.e. 4–20 mA cm^{-2}), the lactic acid is primarily determined by how much of the dihydroxyacetone intermediate is available. The higher the potential, the more intermediate is produced, which corresponds to an increasing trend in lactic acid yield. At high overpotentials (i.e. >24 mA cm^{-2}), the reaction becomes dominated by the electrochemical pathway, and therefore the dehydration towards lactic acid is suppressed. It is noticible that at 36 mA cm^{-2}, towards the end of the electrolysis the cell voltage increased dramatically, possibly due to Pt deactivation from CO-like species poisoning, which is commonly seen in organic compound electroxidation [3]. Therefore, future work is also required to modify the Pt electronic structure to improve the catalyst stability.

Temperature is a crucial parameter in heterogeneous catalysis as it affects the reaction rate and thermodynamics. Additionally, temperature influences the adsorption and desorption of reactants and products on the catalyst surface. Therefore, an increase in temperature will not only improve the diffusion rate of dihydroxyacetone intermediates from the catalyst surface to the electrolyte (resulting in a similar effect as increased mass transport), but also cause the energy levels of the molecules to increase, resulting in a higher rate of the dehydration reaction. Explanations for the effects of temperature on the electrochemical oxidation of glycerol have also been proposed in the literature. According to Fan *et al*, the glycerol oxidation

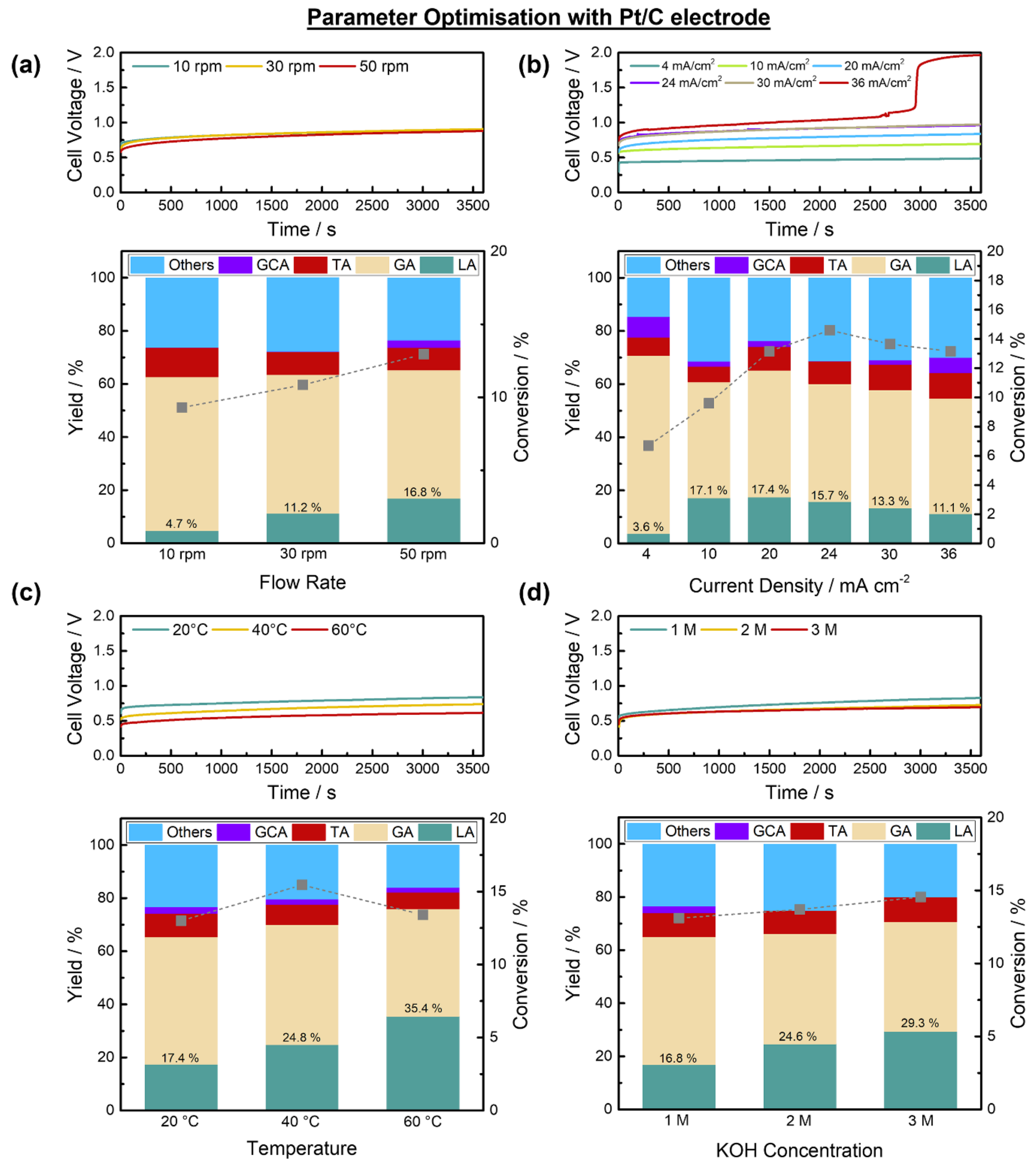

Figure 5. Glycerol electrolysis parameter optimisation with Pt/C electrode: the product yield % (left) and glycerol conversion % (right) results when varying different reaction parameters: (a) flow rate; (b) current density; (c) temperature; (d) KOH concentration. The rest are kept the same as the standard condition. The corresponding electrolysis data are shown above each panel.

reaction is much like thermal activation processes, meaning that higher temperatures have a positive effect on glycerol's reactivity in the reaction [33]. Lee *et al* provide insight on a molecular level, stating that higher temperatures improve glycerol oxidation performance by facilitating the adsorption of OH species onto the catalyst, and consequently the dissociation of O–H and C–H bonds [37].

Finally, the effect of KOH concentrations in tuning the product distribution has also been previously reported for electrochemical glycerol transformation [32, 38]. In our case, this shows that high pH conditions favor the dehydration of dihydroxyacetone more than the competing glyceraldehyde oxidation. Furthermore, the role of KOH in catalysing the Cannizzaro reaction to produce lactic acid from pyruvaldehyde plays a part in improving its corresponding lactic acid yield [16]. Nevertheless, our previous studies on techno-economic analysis and life-cycle assessment of glycerol electrolysis showed that the consumption of alkaline reagents is a large contributing factor in increasing the operational cost and carbon footprint [3]. Therefore, from a practical point of view, in the following investigation, we still chose to use 1 M KOH as the supporting electrolyte.

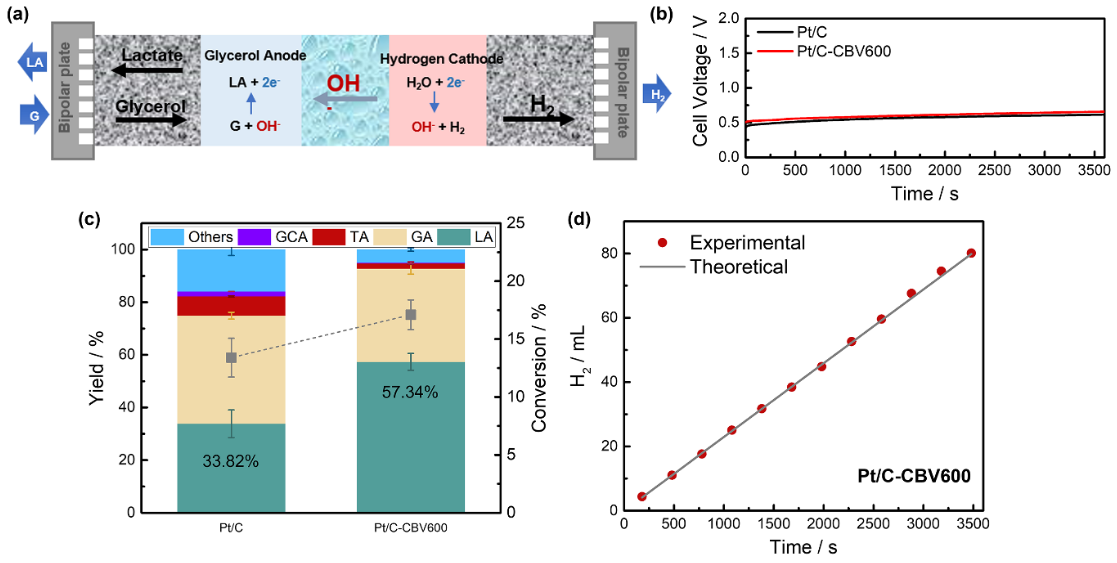

Figure 6. (a) Illustration of the glycerol electrolyser. Comparison of the (b) electrolysis data and (c) product yield % and glycerol conversion rate % of using Pt/C and Pt/C-CBV600 anode. Conditions: current density: 20 mA cm^{-2}, analyte: 1 M glycerol + 1 M KOH, catholyte: 1 M KOH, flow rate: 50 rpm, temperature: 60 °C. For each sample, three independent replicates were conducted. The product yield and conversion rate were calculated based on all three set of results. (d) Experimental and theoretical H_2 production with Pt/C-CBV600 anode (0.1 mg cm^{-2} Pt loading) and Pt/C cathode (0.05 mg cm^{-2} Pt loading). Current density: 40 mA cm^{-2}.

As speculated previously, the Lewis acid sites on the zeolite material surface may serve as active catalytic sites to bind with dihydroxyactone and convert it to lactic acid. Therefore, CBV600 zeolite was used alongside Pt/C to construct a multi-component catalytic system. NH_3-TPD measurements were used to determine the total acid site concentration of the CBV600 catalysts. The Lewis acid site density calculated from the NH_3 desorption at 100 °C is 291 μmol g^{-1}, slightly lower than previously reported values due to the low temperature chosen here [39, 40]. As a comparison, the surface acidity of the carbon black was also measured and calculated to be 18 μmol g^{-1}, which is negligible compared to CBV600. With the above-optimised reaction conditions, the performance of Pt/C and Pt/C-CBV600 catalysts towards glycerol electrolysis were evaluated, and the results are presented in figure 6. The electrolysis cell voltages are very similar when using Pt/C and Pt/C-CBV600 as anodes (figure 6(b)), indicating that the first step, electrochemical glycerol dehydrogenation, happened at similar potential, with similar dihydroxyacetone yields. Yet, the lactic acid yield with Pt/C-CBV600 anode is significantly higher than that of the Pt/C anode, achieving 57.3%. These results demonstrate that the added CBV600 component in the catalyst system is indeed beneficial for promoting the glycerol dehydration pathway and leads to higher lactic acid yield. This could be attributed to the Lewis acid sites on CBV600 surface that help bind the dihydroxyactone intermediate. However, as previous similar studies indicated, the pore structure and surface defects of the catalyst also play important roles in the glycerol conversion [41, 42]. Therefore, these effects need to be investigated in-depth in future work to reveal the detailed promoting role zeolite plays in electrocatalytic glycerol conversion. Subsequently, H_2 production was measured at the same reaction condition with a higher current density of 40 mA cm^{-2}. Over the 1 h electrolysis, the H_2 production stream was steady, and the calculated faradaic efficiency was 99.4%. As shown in figure 6(d), the experimental results match well with the theoretical values calculated with 100% hydrogen evolution reaction faradaic efficiency.

Combining the NH_3-TPD and electrolysis results, we propose that engineering Pt/C-CBV600 multicomponent catalysts can promote the glycerol to lactic acid transformation, due to the modified catalytic microenvironment which induces a tandem reaction effect. In this process, the glycerol dehydrogenation process to form dihydroxyacetone happens electrochemically on the Pt surface, coupled with electron and proton transfer. The dihydroxyacetone will then desorb from the Pt surface, due to the exothermic process, and diffuse to CBV600 zeolite acidic sites, where the species can be adsorbed and activated via a dehydration process, resulting in pyruvaldehyde. The pyruvaldehyde intermediate will then diffuse into the solution and go through Cannizzaro rearrangement, being catalyzed by the OH^- ions and eventually forming lactic acid. The overall process is illustrated in Scheme 1.

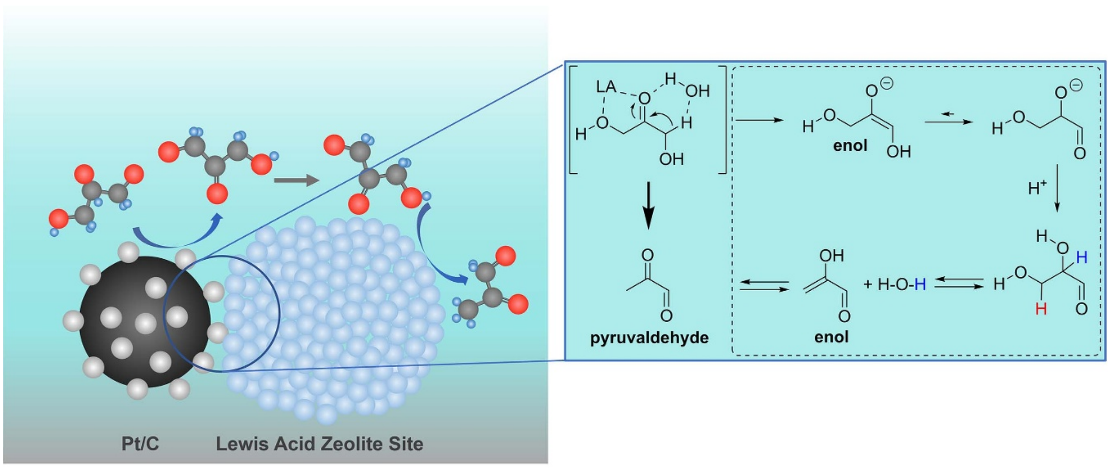

Scheme 1. Illustration of the glycerol → dihydroxyacetone → pyruvaldehyde transformation at Pt/C and zeolite microenvironment interface.

4. Conclusion

The above studies demonstrate that since glycerol to lactic acid transformation is a combined electrochemical and chemical process, it is important to seek solutions that maximise the reactivity for both steps. Although Pt-based materials are currently the state-of-the-art catalyst for the electrochemical step, utilising it standalone cannot achieve high lactic acid yield, due to the competing electrochemical oxidation pathway towards glyceric acid. However, by optimising the reaction conditions and designing suitable catalytic systems, it is possible to break the limit of Pt, and further increase the yield of lactic acid. In this regard, CBV600 zeolite with abundant Lewis acid surface sites can effectively bind the dihydroxyacetone intermediate, and drive the reaction towards pyruvaldehyde heterogeneously. The high mass transport environment provided by increasing the flow rate helps the dihydroxyacetone diffusion from Pt surface to the acidic sites. The elevated temperature promotes the reaction kinetics for both the heterogeneous dihydroxyacetone to pyruvaldehyde transformation, as well as the pyruvaldehyde to lactic acid solution phase reaction. The latter step also benefits from the OH^- ion enriched environment when KOH concentration is increased. We believe that the achievements of an effective multi-component catalyst system of such Pt/C-CBV600 nanostructures will pave the way to the design of highly active and selective catalysts for glycerol electrolysis for the co-production of lactic acid and hydrogen. However, the detailed mechanism of how the Lewis acid sites affect the reaction pathway needs to be investigated, along with the influence of pore structure and surface defects. Therefore, future work will focus on screening multiple different catalyst materials with different acidities and combine theoretical calculations to probe the selectivity descriptors. Since Pt deactivation due to CO-like species poisoning and particle dissolution.

Data availability statement

The data cannot be made publicly available upon publication because they contain commercially sensitive information. The data that support the findings of this study are available upon reasonable request from the authors.

Acknowledgments

The work was supported by a donation from Mr Mark Richardson to the Department of Chemical Engineering at Imperial College London. H L thank Professor Magda Titirici for providing the lab equipment. M N G and D C A thank PID2021-123079OB-I00 Project Funded by MCIN/AEI/10.13039/501100011033 and 'ERDF A way of making Europe'.

Conflict of interest

There are no conflicts to declare.

ORCID iD

Hui Luo https://orcid.org/0000-0002-5876-0294

References

[1] Garlyyev B, Xue S, Fichtner J, Bandarenka A S and Andronescu C 2020 Prospects of value-added chemicals and hydrogen via electrolysis *ChemSusChem* **13** 2513–21

[2] Tang C, Zheng Y, Jaroniec M and Qiao S Z 2021 Electrocatalytic refinery for sustainable production of fuels and chemicals *Angew. Chem., Int. Ed.* **60** 19572–90

[3] Luo H, Barrio J, Sunny N, Li A, Steier L, Shah N, Stephens I E L and Titirici M-M 2021 Progress and perspectives in photo- and electrochemical-oxidation of biomass for sustainable chemicals and hydrogen production *Adv. Energy Mater.* **11** 2101180

[4] Dodekatos G, Schünemann S and Tüysüz H 2018 Recent advances in thermo-, photo-, and electrocatalytic glycerol oxidation *ACS Catal.* **8** 6301–33

[5] Pagliaro M, Ciriminna R, Kimura H, Rossi M and Della Pina C 2007 From glycerol to value-added products *Angew. Chem., Int. Ed.* **46** 4434–40

[6] Simões M, Baranton S and Coutanceau C 2012 Electrochemical valorisation of glycerol *ChemSusChem* **5** 2106–24

[7] Monteiro M R, Kugelmeier C L, Pinheiro R S, Batalha M O and da Silva César A 2018 Glycerol from biodiesel production: technological paths for sustainability *Renew. Sustain. Energy Rev.* **88** 109–22

[8] Lari G M, Pastore G, Haus M, Ding Y, Papadokonstantakis S, Mondelli C and Pérez-Ramírez J 2018 Environmental and economical perspectives of a glycerol biorefinery *Energy Environ. Sci.* **11** 1012–29

[9] Abdel-Rahman M A, Tashiro Y and Sonomoto K 2013 Recent advances in lactic acid production by microbial fermentation processes *Biotechnol. Adv.* **31** 877–902

[10] Tu Q, Parvatker A, Garedew M, Harris C, Eckelman M, Zimmerman J B, Anastas P T and Lam C H 2021 Electrocatalysis for chemical and fuel production: investigating climate change mitigation potential and economic feasibility *Environ. Sci. Technol.* **55** 3240–9

[11] John R P, Nampoothiri K M and Pandey A 2007 Fermentative production of lactic acid from biomass: an overview on process developments and future perspectives *Appl. Microbiol. Biotechnol.* **74** 524–34

[12] Dusselier M, Van Wouwe P, Dewaele A, Makshina E and Sels B F 2013 Lactic acid as a platform chemical in the biobased economy: the role of chemocatalysis *Energy Environ. Sci.* **6** 1415–42

[13] Morales M, Dapsens P Y, Giovinazzo I, Witte J, Mondelli C, Papadokonstantakis S, Hungerbühler K and Pérez-Ramírez J 2015 Environmental and economic assessment of lactic acid production from glycerol using cascade bio- and chemocatalysis *Energy Environ. Sci.* **8** 558–67

[14] Purushothaman R K P, van Haveren J, van Es D S, Melián-Cabrera I, Meeldijk J D and Heeres H J 2014 An efficient one pot conversion of glycerol to lactic acid using bimetallic gold-platinum catalysts on a nanocrystalline CeO_2 support *Appl. Catal.* B **147** 92–100

[15] Shen Y, Zhang S, Li H, Ren Y and Liu H 2010 Efficient synthesis of lactic acid by aerobic oxidation of glycerol on Au-Pt/TiO_2 catalysts *Chemistry* A **16** 7368–71

[16] Dai C, Sun L, Liao H, Khezri B, Webster R D, Fisher A C and Xu Z J 2017 Electrochemical production of lactic acid from glycerol oxidation catalyzed by AuPt nanoparticles *J. Catal.* **356** 14–21

[17] Lux S and Siebenhofer M 2013 Synthesis of lactic acid from dihydroxyacetone: use of alkaline-earth metal hydroxides *Catal. Sci. Technol.* **3** 1380–5

[18] Albuquerque E M, Borges L E P, Fraga M A and Sievers C 2017 Relationship between Acid–Base properties and the activity of ZrO_2-based catalysts for the cannizzaro reaction of pyruvaldehyde to lactic acid *ChemCatChem* **9** 2675–83

[19] Kwon Y, Schouten K J P and Koper M T M 2011 Mechanism of the catalytic oxidation of glycerol on polycrystalline gold and platinum electrodes *ChemCatChem* **3** 1176–85

[20] Li T and Harrington D A 2021 An overview of glycerol electrooxidation mechanisms on Pt, Pd and Au *ChemSusChem* **14** 1472–95

[21] Brix A C *et al* 2021 Electrocatalytic oxidation of glycerol using solid-state synthesised nickel boride: impact of key electrolysis parameters on product selectivity *ChemElectroChem* **8** 2336–42

[22] Albuquerque E M, Borges L E P and Fraga M A 2015 Lactic acid production from aqueous-phase selective oxidation of hydroxyacetone *J. Mol. Catal.* A **400** 64–70

[23] Pescarmona P P, Janssen K P F, Delaet C, Stroobants C, Houthoofd K, Philippaerts A, De Jonghe C, Paul J S, Jacobs P A and Sels B F 2010 Zeolite-catalysed conversion of C3 sugars to alkyl lactates *Green Chem.* **12** 1083–9

[24] West R M, Holm M S, Saravanamurugan S, Xiong J, Beversdorf Z, Taarning E and Christensen C H 2010 Zeolite H-USY for the production of lactic acid and methyl lactate from C3-sugars *J. Catal.* **269** 122–30

[25] Iglesias J *et al* 2020 Advances in catalytic routes for the production of carboxylic acids from biomass: a step forward for sustainable polymers *Chem. Soc. Rev.* **49** 5704–71

[26] Rasrendra C B, Fachri B A, Makertihartha I G B N, Adisasmito S and Heeres H J 2011 Catalytic conversion of dihydroxyacetone to lactic acid using metal salts in water *ChemSusChem* **4** 768–77

[27] Wang X, de Araújo J F, Ju W, Bagger A, Schmies H, Kühl S, Rossmeisl J and Strasser P 2019 Mechanistic reaction pathways of enhanced ethylene yields during electroreduction of CO_2–CO co-feeds on Cu and Cu-tandem electrocatalysts *Nat. Nanotechnol.* **14** 1063–70

[28] Morales-Guio C G *et al* 2018 Improved CO_2 reduction activity towards C_{2+} alcohols on a tandem gold on copper electrocatalyst *Nat. Catal.* **1** 764–71

[29] Chen C, Li Y, Yu S, Louisia S, Jin J, Li M, Ross M B and Yang P 2020 Cu-Ag tandem catalysts for high-rate CO_2 electrolysis toward multicarbons *Joule* **4** 1688–99

[30] Yu S, Louisia S and Yang P 2022 The interactive dynamics of nanocatalyst structure and microenvironment during electrochemical CO_2 conversion *JACS Au* **2** 562–72

[31] Lum Y and Ager J W 2018 Sequential catalysis controls selectivity in electrochemical CO_2 reduction on Cu *Energy Environ. Sci.* **11** 2935–44

[32] Qi J, Xin L, Chadderdon D J, Qiu Y, Jiang Y, Benipal N, Liang C and Li W 2014 Electrocatalytic selective oxidation of glycerol to tartronate on Au/C anode catalysts in anion exchange membrane fuel cells with electricity cogeneration *Appl. Catal.* B **154–155** 360–8

[33] Fan L, Liu B, Liu X, Senthilkumar N, Wang G and Wen Z 2021 Recent progress in electrocatalytic glycerol oxidation *Energy Technol.* **9** 2000804

[34] Melle G, de Souza M B C, Santiago P V B, Corradini P G, Mascaro L H, Fernández P S and Sitta E 2021 Glycerol electro-oxidation at Pt in alkaline media: influence of mass transport and cations *Electrochim. Acta* **398** 139318

[35] Lam C H, Bloomfield A J and Anastas P T 2017 A switchable route to valuable commodity chemicals from glycerol via electrocatalytic oxidation with an earth abundant metal oxidation catalyst *Green Chem.* **19** 1958–68

[36] Roquet L, Belgsir E M, Léger J-M and Lamy C 1994 Kinetics and mechanisms of the electrocatalytic oxidation of glycerol as investigated by chromatographic analysis of the reaction products: potential and pH effects *Electrochim. Acta* **39** 2387–94

[37] Lee C S, Aroua M K, Wan Daud W A, Cognet P, Pérès Y and Ajeel M A 2019 Selective electrochemical conversion of glycerol to glycolic acid and lactic acid on a mixed carbon-black activated carbon electrode in a single compartment electrochemical cell *Front. Chem.* **7** 110

[38] Lux S, Stehring P and Siebenhofer M 2010 Lactic acid production as a new approach for exploitation of glycerol *Sep. Sci. Technol.* **45** 1921–7

[39] Chung K H *et al* 2017 Highly selective catalytic properties of HZSM-5 zeolite in the synthesis of acetyl triethyl citrate by the acetylation of triethyl citrate with acetic anhydride *Catalysts* **7** 321

[40] Ribeiro S P, da S, Barbosa G M, Rocha M A D F, Landesmann A, Nascimento M A C and Nascimento R S V 2020 Influence of the zeolite acidity on its synergistic action with a flame-retarding polymeric intumescent formulation *J. Mater. Sci.* **55** 619–30

[41] Vu H T, Harth F M, Goepel M, Linares N, García–Martínez J and Gläser R 2022 Enhanced activity of a bifunctional Pt/zeolite Y catalyst with an intracrystalline hierarchical pore system in the aqueous-phase hydrogenation of levulinic acid *Chem. Eng. J.* **430** 132763

[42] Anil A, White J, Campos Dos Santos E, Terekhina I, Johnsson M, Pettersson L G M, Cornell A and Salazar-Alvarez G 2023 Effect of pore mesostructure on the electrooxidation of glycerol on Pt mesoporous catalysts *J. Mater. Chem.* A **11** 16570–7